



Received 22 January 2020
Accepted 10 February 2020

Edited by C. Rizzoli, Universita degli Studi di Parma, Italy

Keywords: crystal structure; charge assisted hydrogen bonding; thiazolidine ring; envelope conformation; Hirshfeld surface analysis.

CCDC reference: 1837123

Supporting information: this article has supporting information at journals.iucr.org/e

Crystal structure and Hirshfeld surface analysis of (*E*)-3-(benzylideneamino)-5-phenylthiazolidin-2-iminium bromide

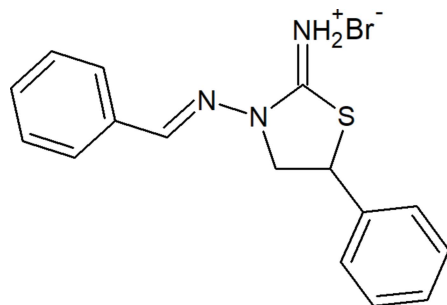
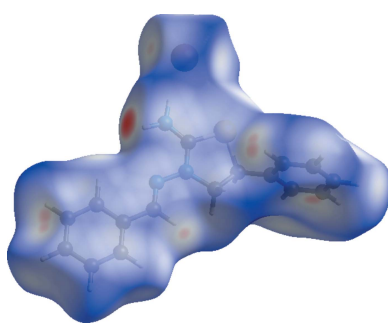
Gulnara Sh. Duruskari,^a Mehmet Akkurt,^b Gunay Z. Mammadova,^a Taras Chyrka^{c*} and Abel M. Maharramov^a

^aOrganic Chemistry Department, Baku State University, Z. Xalilov str. 23, Az, 1148 Baku, Azerbaijan, ^bDepartment of Physics, Faculty of Sciences, Erciyes University, 38039 Kayseri, Turkey, and ^cDepartment of Theoretical and Industrial Heat Engineering (TPT), National Technical University of Ukraine "Igor Sikorsky Kyiv Polytechnic Institute", 03056, Kyiv, Ukraine. *Correspondence e-mail: mustford@ukr.net

The central thiazolidine ring of the title salt, $C_{16}H_{16}N_3S^+\cdot Br^-$, adopts an envelope conformation, with the C atom bearing the phenyl ring as the flap atom. In the crystal, the cations and anions are linked by N—H···Br hydrogen bonds, forming chains parallel to the *b*-axis direction. Hirshfeld surface analysis and two-dimensional fingerprint plots indicate that the most important contributions to the crystal packing are from H···H (46.4%), C···H/H···C (18.6%) and H···Br/Br···H (17.5%) interactions.

1. Chemical context

Sulfur and nitrogen-containing heterocycles maintain their importance as key fragments of drugs and medicinally active compounds (Pathania *et al.*, 2019). Moreover, azomethine-containing structural motifs have been widely employed for industrial purposes as they exhibit a broad range of biological activities, and are used in synthesis, catalysis and the design of materials (Gurbanov *et al.*, 2017, 2018; Mahmoudi *et al.*, 2018a,b,c; Mamedov *et al.*, 2018). Nowadays, N-ligands are key players in a wide diversity of fields, namely in coordination, metal–organic, pharmaceutical and medicinal chemistry, biologically active compounds, catalysis, non-covalent interactions and supramolecular assemblies (Maharramov *et al.*, 2011, 2018; Mahmudov *et al.*, 2013, 2014, 2017a,b, 2019; Mamedov *et al.*, 2015). In our previous studies we have reported on the molecular structural properties of a series of 5-phenylthiazolidin-2-imine derivatives (Akkurt *et al.*, 2018a,b; Duruskari *et al.*, 2019a,b; Khalilov *et al.*, 2019; Maharramov *et al.*, 2019). Following further study in this field, herein we report the crystal structure and Hirshfeld surface analysis of the title compound, (*E*)-3-(benzylideneamino)-5-phenylthiazolidin-2-iminium bromide.



OPEN ACCESS

Table 1
Hydrogen-bond geometry (\AA , $^\circ$).

$D-\text{H}\cdots A$	$D-\text{H}$	$\text{H}\cdots A$	$D\cdots A$	$D-\text{H}\cdots A$
N3—H3A···Br1	0.90	2.37	3.258 (3)	168
N3—H3B···Br1 ⁱ	0.90	2.55	3.399 (3)	158

Symmetry code: (i) $-x + 1, y + \frac{1}{2}, -z + \frac{3}{2}$.

2. Structural commentary

The thiazolidine ring (S1/N2/C1—C3) in the cation of the title salt (Fig. 1) adopts an envelope conformation, with the C atom bearing the phenyl ring as the flap atom; the puckering parameters are $Q(2) = 0.318 (3)$ \AA and $\varphi(2) = 42.0 (5)$ $^\circ$. The mean plane of the thiazolidine ring makes dihedral angles of 18.28 (15) and 83.19 (15) $^\circ$, respectively, with the C5—C10 and C11—C16 phenyl rings of the 3-(benzylideneamino) and 5-phenylthiazolidin groups, while the dihedral angle between them is 82.54 (15) $^\circ$. The torsion angle of the N2—N1—C4—C5 bridge that links the thiazolidine and 3-(benzylideneamino) units is $-175.7 (3)$ $^\circ$.

3. Supramolecular features

In the crystal, adjacent cations and anions are linked by pairs of $\text{N}-\text{H}\cdots\text{Br}$ hydrogen bonds (Table 1, Fig. 2), forming chains running parallel to the b -axis direction. $\text{C}-\text{H}\cdots\pi$ interactions or $\pi-\pi$ stacking interactions contributing to the stabilization of the crystal packing are not observed.

4. Hirshfeld surface analysis

The Hirshfeld surface analysis (Spackman & Jayatilaka, 2009) of the title compound was generated by *CrystalExplorer 3.1* (Wolff *et al.*, 2012), and comprises d_{norm} surface plots and two-dimensional fingerprint plots (Spackman & McKinnon, 2002). A d_{norm} surface plot of the title compound mapped over d_{norm}

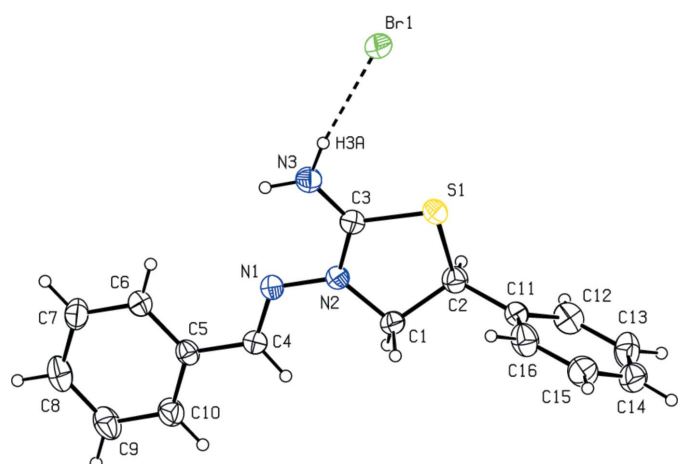


Figure 1

The molecular structure of the title salt, with the atom labelling. Displacement ellipsoids are drawn at the 30% probability level. The interionic hydrogen bond is shown as a dashed line.

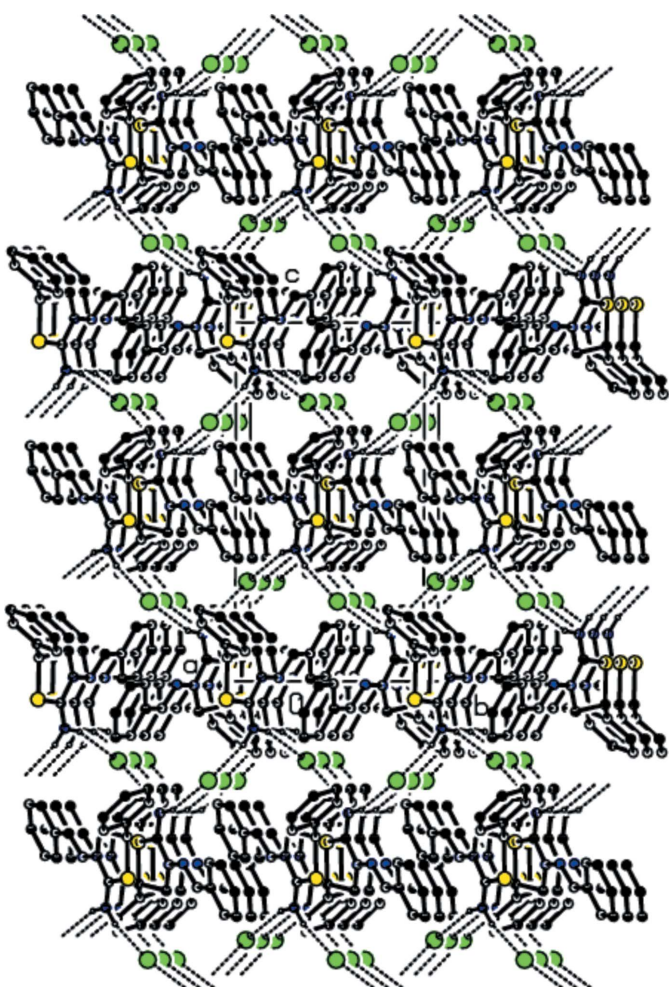


Figure 2

A view of the crystal packing showing the formation of chains parallel to the b axis through $\text{N}-\text{H}\cdots\text{Br}$ hydrogen bonds (dashed lines).

using a standard surface resolution with a fixed colour scale of -0.3485 (red) to 1.3503 a.u. (blue) is shown in Fig. 3. The dark-red spots on the d_{norm} surface arise as a result of short inter-

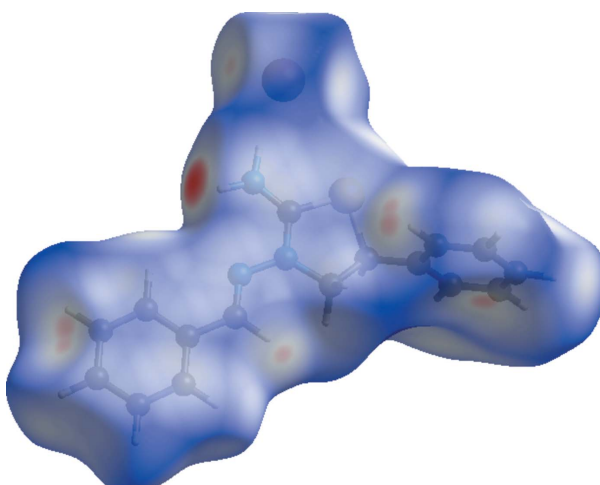


Figure 3

View of the three-dimensional Hirshfeld surface of the title salt plotted over d_{norm} .

Table 2Summary of short interatomic contacts (\AA) in the title salt.

Contact	Distance	Symmetry operation
Br1 \cdots H3A (N3)	2.37	x, y, z
Br1 \cdots H3B (N3)	2.55	$1 - x, -\frac{1}{2} + y, \frac{3}{2} - z$
Br1 \cdots H14A (C14)	3.14	$-x, 1 - y, 1 - z$
Br1 \cdots H4A (C4)	2.96	$x, \frac{3}{2} - y, \frac{1}{2} + z$
Br1 \cdots H12A (C12)	3.02	$x, \frac{1}{2} - y, \frac{1}{2} + z$

atomic contacts (Table 2), while the other weaker intermolecular interactions appear as light-red spots.

The shape index of the Hirshfeld surface is a tool to visualize $\pi\cdots\pi$ stacking interactions by the presence of adjacent red and blue triangles; if there are no adjacent red and/or blue triangles, then there are no $\pi\cdots\pi$ interactions. Fig. 4 clearly suggests that there are no $\pi\cdots\pi$ interactions present in the title compound. Fig. 5(a) shows the two-dimensional fingerprint of the sum of the contacts contributing to the Hirshfeld surface represented in normal mode (Tables 1 and 2). The fingerprint plots delineated into H \cdots H (46.4%), C \cdots H/H \cdots C (18.6%), H \cdots Br/Br \cdots H (17.5%), H \cdots S/S \cdots H (4.5%) and C \cdots N/N \cdots C (3.7%) contacts are shown in Fig. 5b–f.

The most significant intermolecular interactions are the H \cdots H interactions (46.4%) (Fig. 5b). All of the contributions to the Hirshfeld surface are given in Table 3. The large number of H \cdots H, C \cdots H/H \cdots C and H \cdots Br/Br \cdots H interactions suggest that van der Waals interactions and hydrogen bonding play the major roles in the crystal packing (Hathwar *et al.*, 2015).

5. Database survey

A search of the Cambridge Structural Database (CSD, Version 5.40, February 2019; Groom *et al.*, 2016) for 2-thiazolidiniminium compounds gave ten hits, *viz.* MOJGUQ (Duruskari *et al.*, 2019a), XOWXAL (Duruskari *et al.*, 2019b), BOBWIB (Khalilov *et al.*, 2019), UDELUN (Akkurt *et al.*, 2018a), WILBIC (Marthi *et al.*, 1994), WILBOI (Marthi *et al.*,

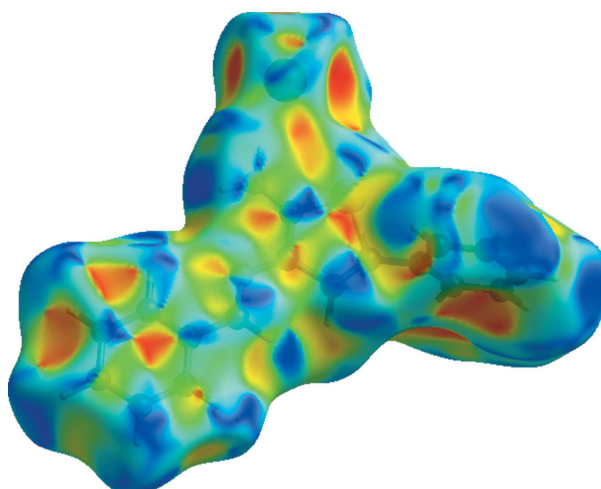


Figure 4
Hirshfeld surface of the title salt plotted over shape-index.

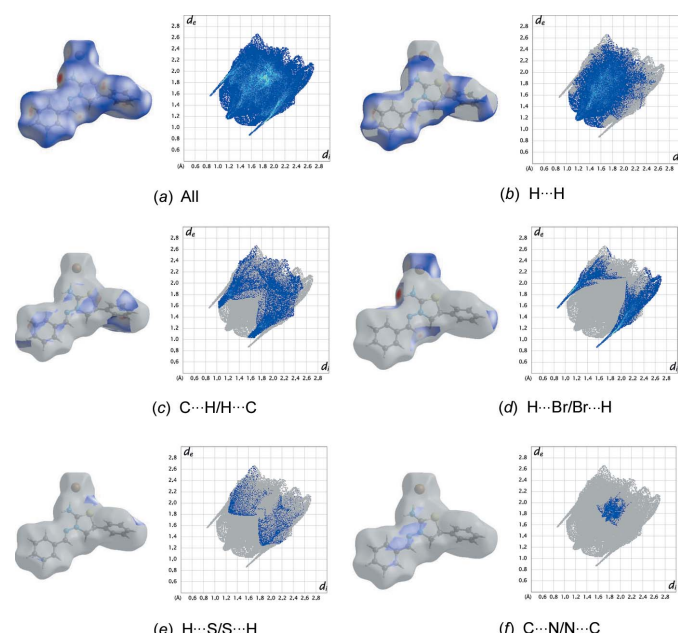
Table 3

Percentage contributions of interatomic contacts to the Hirshfeld surface for the title salt.

Contact	Percentage contribution
H \cdots H	46.4
C \cdots H/H \cdots C	18.6
H \cdots Br/Br \cdots H	17.5
H \cdots S/S \cdots H	4.5
C \cdots N/N \cdots C	3.7
C \cdots S/S \cdots C	3.0
H \cdots N/N \cdots H	2.6
C \cdots C	2.3
C \cdots Br/Br \cdots C	0.9
N \cdots S/S \cdots N	0.5
N \cdots N	0.2

1994), WILBOI01 (Marthi *et al.*, 1994), YITCEJ (Martem'yanova *et al.*, 1993a), YITCAF (Martem'yanova *et al.*, 1993b) and YOPLUK (Marthi *et al.*, 1995).

In the crystal of MOJGUQ (Duruskari *et al.*, 2019a), centrosymmetrically related cations and anions are linked into dimeric units *via* N \cdots H \cdots Br hydrogen bonds, which are further connected by weak C \cdots H \cdots Br contacts into chains parallel to the *a* axis. Furthermore, C \cdots H \cdots π interactions and $\pi\cdots\pi$ stacking interactions [centroid-to-centroid distance = 3.897 (2) \AA] between the major components of the disordered phenyl ring contribute to the stabilization of the molecular packing. In the crystal of XOWXAL (Duruskari *et al.*, 2019b), the thiazolidine ring adopts an envelope conformation. N \cdots H \cdots Br hydrogen bonds link the components into a three-dimensional network. Weak $\pi\cdots\pi$ stacking interactions

**Figure 5**

The Hirshfeld surface representations and the full two-dimensional fingerprint plots for the title salt, showing (a) all interactions, and delineated into (b) H \cdots H, (c) C \cdots H/H \cdots C, (d) H \cdots Br/Br \cdots H, (e) H \cdots S/S \cdots H and (f) C \cdots N/N \cdots C interactions. The d_i and d_e values are the closest internal and external distances (in \AA) from given points on the Hirshfeld surface.

Table 4
Experimental details.

Crystal data	
Chemical formula	$C_{16}H_{16}N_3S^+\cdot Br^-$
M_r	362.29
Crystal system, space group	Monoclinic, $P2_1/c$
Temperature (K)	296
a, b, c (Å)	12.138 (8), 8.336 (5), 15.872 (9)
β (°)	93.910 (16)
V (Å ³)	1602.3 (17)
Z	4
Radiation type	Mo $K\alpha$
μ (mm ⁻¹)	2.69
Crystal size (mm)	0.21 × 0.18 × 0.13
Data collection	
Diffractometer	Bruker APEXII CCD
Absorption correction	Multi-scan (<i>SADABS</i> ; Bruker, 2003)
T_{min}, T_{max}	0.582, 0.713
No. of measured, independent and observed [$I > 2\sigma(I)$] reflections	23979, 3314, 2742
R_{int}	0.049
(sin θ/λ) _{max} (Å ⁻¹)	0.629
Refinement	
$R[F^2 > 2\sigma(F^2)]$, $wR(F^2)$, S	0.040, 0.111, 1.06
No. of reflections	3314
No. of parameters	190
No. of restraints	12
H-atom treatment	H-atom parameters constrained
$\Delta\rho_{\max}, \Delta\rho_{\min}$ (e Å ⁻³)	0.74, -0.60

Computer programs: *APEX2* and *SAINT* (Bruker, 2003), *SHELXT2014* (Sheldrick, 2015a), *SHELXL2016* (Sheldrick, 2015b) and *SHELXTL* (Sheldrick, 2008).

between the phenyl rings of adjacent cations also contribute to the molecular packing. In the crystal of BOBWIB (Khalilov *et al.*, 2019), the central thiazolidine ring adopts an envelope conformation. In the crystal, centrosymmetrically related cations and anions are linked into dimeric units *via* N—H···Br hydrogen bonds, which are further connected by weak C—H···Br hydrogen bonds into chains parallel to [110]. In the crystal of UDELUN (Akkurt *et al.*, 2018a), C—H···Br and N—H···Br hydrogen bonds link the components into a three-dimensional network with the cations and anions stacked along the *b*-axis direction. Weak C—H···π interactions, which only involve the minor disorder component of the ring, also contribute to the molecular packing. In addition, there are also inversion-related Cl···Cl halogen bonds and C—Cl···π(ring) contacts. In the other structures, the 3-N atom carries a C-substituent instead of an N-substituent as found in the title compound. Three of them were determined to be racemic (WILBIC; Marthi *et al.*, 1994) and two optically active samples (WILBOI and WILBOI01; Marthi *et al.*, 1994) of 3-(2'-chloro-2'-phenylethyl)-2-thiazolidiniminium *p*-toluenesulfonate. In all three structures, the most disordered fragment is the asymmetric C atom and the Cl atom attached to it. The disorder of the cation in the racemate corresponds to the presence of both enantiomers at each site in the ratio 0.821 (3):0.179 (3). The system of hydrogen bonds connecting two cations and two anions into 12-membered rings is identical in the racemic and in the optically active crystals. YITCEJ (Martem'yanova *et al.*, 1993a), is a product of the interaction

of 2-amino-5-methylthiazoline with methyl iodide, with alkylation at the endocyclic nitrogen atom, while YITCAF (Martem'yanova *et al.*, 1993b) is a product of the reaction of 3-nitro-5-methoxy-, 3-nitro-5-chloro-, and 3-bromo-5-nitro-salicylaldehyde with the heterocyclic base to form the salt-like complexes.

6. Synthesis and crystallization

To the solution of 3-amino-5-phenylthiazolidin-2-iminium bromide (1 mmol) in 20 mL of ethanol was added benzaldehyde (1 mmol) and the mixture was refluxed for 2 h. After cooling down to room temperature, the reaction product precipitated as colourless single crystals, which were collected by filtration and washed with cold acetone (yield 76%), m.p. 519 K. Analysis calculated for $C_{16}H_{16}BrN_3S$ ($M_r = 362.29$): C, 53.04; H, 4.45; N, 11.60. Found: C, 53.01; H, 4.42; N, 11.56%. ¹H NMR (300 MHz, DMSO-*d*₆) : 4.58 (*k*, 1H, CH₂, ³J_{H-H} = 6.9); 4.89 (*t*, 1H, CH₂, ³J_{H-H} = 8.1); 5.60 (*t*, 1H, CH-Ar, ³J_{H-H} = 7.5); 7.37–8.07 (*m*, 10H, 10Ar-H); 8.44 (*s*, 1H, CH=), 10.35 (*s*, 2H, NH=). ¹³C NMR (75 MHz, DMSO-*d*₆): 45.36, 55.91, 127.76, 128.65, 128.82, 128.86, 129.09, 131.54, 132.85, 137.48, 151.11, 167.84. MS (ESI), *m/z*: 282.30 [$C_{16}H_{16}N_3S$]⁺ and 79.88 Br⁻.

7. Refinement

Crystal data, data collection and structure refinement details are summarized in Table 4. All H atoms were placed at calculated positions (N—H = 0.90 Å and C—H = 0.93–0.98 Å) and refined using a riding model, with $U_{iso}(H) = 1.2U_{eq}(N, C)$. The distances between the carbon atoms of two phenyl groups were constrained with a DFIX instruction [DFIX 1.40 0.02 C C].

References

- Akkurt, M., Duruskari, G. S., Toze, F. A. A., Khalilov, A. N. & Huseynova, A. T. (2018a). *Acta Cryst.* **E74**, 1168–1172.
- Akkurt, M., Maharramov, A. M., Duruskari, G. S., Toze, F. A. A. & Khalilov, A. N. (2018b). *Acta Cryst.* **E74**, 1290–1294.
- Bruker (2003). *APEX2*, *SAINT* and *SADABS*. Bruker AXS Inc., Madison, Wisconsin, USA.
- Duruskari, G. S., Khalilov, A. N., Akkurt, M., Mammadova, G. Z., Chyrka, T. & Maharramov, A. M. (2019a). *Acta Cryst.* **E75**, 1544–1547.
- Duruskari, G. S., Khalilov, A. N., Akkurt, M., Mammadova, G. Z., Chyrka, T. & Maharramov, A. M. (2019b). *Acta Cryst.* **E75**, 1175–1179.
- Groom, C. R., Bruno, I. J., Lightfoot, M. P. & Ward, S. C. (2016). *Acta Cryst.* **B72**, 171–179.
- Gurbanov, A. V., Maharramov, A. M., Zubkov, F. I., Saifutdinov, A. M. & Guseinov, F. I. (2018). *Aust. J. Chem.* **71**, 190–194.
- Gurbanov, A. V., Mahmudov, K. T., Kopylovich, M. N., Guedes da Silva, F. M., Sutradhar, M., Guseinov, F. I., Zubkov, F. I., Maharramov, A. M. & Pombeiro, A. J. L. (2017). *Dyes Pigments*, **138**, 107–111.
- Hathwar, V. R., Sist, M., Jørgensen, M. R. V., Mamakhe, A. H., Wang, X., Hoffmann, C. M., Sugimoto, K., Overgaard, J. & Iversen, B. B. (2015). *IUCrJ*, **2**, 563–574.
- Khalilov, A. N., Atioğlu, Z., Akkurt, M., Duruskari, G. S., Toze, F. A. A. & Huseynova, A. T. (2019). *Acta Cryst.* **E75**, 662–666.

- Maharramov, A. M., Duruskari, G. Sh., Mammadova, G. Z., Khalilov, A. N., Aslanova, J. M., Cisterna, J., Cárdenas, A. & Brito, I. (2019). *J. Chil. Chem. Soc.* **64**, 4441–4447.
- Maharramov, A. M., Khalilov, A. N., Gurbanov, A. V., Allahverdiyev, M. A. & Ng, S. W. (2011). *Acta Cryst. E* **67**, o721.
- Maharramov, A. M., Shikhaliyev, N. Q., Suleymanova, G. T., Gurbanov, A. V., Babayeva, G. V., Mammadova, G. Z., Zubkov, F. I., Nenajdenko, V. G., Mahmudov, K. T. & Pombeiro, A. J. L. (2018). *Dyes Pigments*, **159**, 135–141.
- Mahmoudi, G., Seth, S. K., Bauzá, A., Zubkov, F. I., Gurbanov, A. V., White, J., Stilinović, V., Doert, Th. & Frontera, A. (2018c). *CrystEngComm*, **20**, 2812–2821.
- Mahmoudi, G., Zangrando, E., Mitoraj, M. P., Gurbanov, A. V., Zubkov, F. I., Moosavifar, M., Konyaeva, I. A., Kirillov, A. M. & Safin, D. A. (2018a). *New J. Chem.* **42**, 4959–4971.
- Mahmoudi, G., Zaręba, J. K., Gurbanov, A. V., Bauzá, A., Zubkov, F. I., Kubicki, M., Stilinović, V., Kinzhybalo, V. & Frontera, A. (2018b). *Eur. J. Inorg. Chem.* pp. 4763–4772.
- Mahmudov, K. T., Gurbanov, A. V., Guseinov, F. I. & Guedes da Silva, M. F. C. (2019). *Coord. Chem. Rev.* **387**, 32–46.
- Mahmudov, K. T., Kopylovich, M. N., Guedes da Silva, M. F. C. & Pombeiro, A. J. L. (2017a). *Dalton Trans.* **46**, 10121–10138.
- Mahmudov, K. T., Kopylovich, M. N., Guedes da Silva, M. F. C. & Pombeiro, A. J. L. (2017b). *Coord. Chem. Rev.* **345**, 54–72.
- Mahmudov, K. T., Kopylovich, M. N., Maharramov, A. M., Kurbanova, M. M., Gurbanov, A. V. & Pombeiro, A. J. L. (2014). *Coord. Chem. Rev.* **265**, 1–37.
- Mahmudov, K. T., Kopylovich, M. N. & Pombeiro, A. J. L. (2013). *Coord. Chem. Rev.* **257**, 1244–1281.
- Mamedov, I. G., Bayramov, M. R., Salanova, A. E. & Maharramov, A. M. (2015). *Indian J. Chem.* **54B**, 1518–1527.
- Mamedov, I. G., Farzaliyeva, A. E., Mamedova, Y. V., Hasanova, N. N., Bayramov, M. R. & Maharramov, A. M. (2018). *Indian J. Chem.* **57B**, 1310–1314.
- Martem'yanova, N. A., Chunaev, Y. M., Przhiyalgovskaya, N. M., Kurkovskaya, L. N., Filipenko, O. S. & Aldoshin, S. M. (1993a). *Khim. Geterotsikl. Soedin.* pp. 415–419.
- Martem'yanova, N. A., Chunaev, Y. M., Przhiyalgovskaya, N. M., Kurkovskaya, L. N., Filipenko, O. S. & Aldoshin, S. M. (1993b). *Khim. Geterotsikl. Soedin.* pp. 420–425.
- Marthi, K., Larsen, M., Ács, M., Bálint, J. & Fogassy, E. (1995). *Acta Chem. Scand.* **49**, 20–27.
- Marthi, K., Larsen, S., Ács, M., Bálint, J. & Fogassy, E. (1994). *Acta Cryst.* **B50**, 762–771.
- Pathania, S., Narang, R. K. & Rawal, R. K. (2019). *Eur. J. Med. Chem.* **180**, 486–508.
- Sheldrick, G. M. (2008). *Acta Cryst. A* **64**, 112–122.
- Sheldrick, G. M. (2015a). *Acta Cryst. A* **71**, 3–8.
- Sheldrick, G. M. (2015b). *Acta Cryst. C* **71**, 3–8.
- Spackman, M. A. & McKinnon, J. J. (2002). *CrystEngComm*, **4**, 378–392.
- Spackman, M. & Jayatilaka, D. (2009). *CrystEngComm*, **11**, 19–32.
- Wolff, S. K., Grimwood, D. J., McKinnon, J. J., Turner, M. J., Jayatilaka, D. & Spackman, M. A. (2012). *Crystal Explorer*. University of Western Australia.

supporting information

Acta Cryst. (2020). E76, 427-431 [https://doi.org/10.1107/S2056989020001899]

Crystal structure and Hirshfeld surface analysis of (*E*)-3-(benzylideneamino)-5-phenylthiazolidin-2-iminium bromide

Gulnara Sh. Duruskari, Mehmet Akkurt, Gunay Z. Mammadova, Taras Chyrka and Abel M. Maharramov

Computing details

Data collection: *APEX2* (Bruker, 2003); cell refinement: *SAINT* (Bruker, 2003); data reduction: *SAINT* (Bruker, 2003); program(s) used to solve structure: *SHELXT2014* (Sheldrick, 2015a); program(s) used to refine structure: *SHELXL2016* (Sheldrick, 2015b); molecular graphics: *SHELXTL* (Sheldrick, 2008); software used to prepare material for publication: *SHELXTL* (Sheldrick, 2008).

(*E*)-3-(Benzylideneamino)-5-phenylthiazolidin-2-iminium bromide

Crystal data

$C_{16}H_{16}N_3S^+\cdot Br^-$
 $M_r = 362.29$
Monoclinic, $P2_1/c$
 $a = 12.138 (8)$ Å
 $b = 8.336 (5)$ Å
 $c = 15.872 (9)$ Å
 $\beta = 93.910 (16)^\circ$
 $V = 1602.3 (17)$ Å³
 $Z = 4$

$F(000) = 736$
 $D_x = 1.502$ Mg m⁻³
Mo $K\alpha$ radiation, $\lambda = 0.71073$ Å
Cell parameters from 9891 reflections
 $\theta = 2.8\text{--}26.4^\circ$
 $\mu = 2.69$ mm⁻¹
 $T = 296$ K
Plate, colourless
0.21 × 0.18 × 0.13 mm

Data collection

Bruker APEXII CCD
diffractometer
 φ and ω scans
Absorption correction: multi-scan
(SADABS; Bruker, 2003)
 $T_{\min} = 0.582$, $T_{\max} = 0.713$
23979 measured reflections

3314 independent reflections
2742 reflections with $I > 2\sigma(I)$
 $R_{\text{int}} = 0.049$
 $\theta_{\max} = 26.5^\circ$, $\theta_{\min} = 2.6^\circ$
 $h = -15 \rightarrow 15$
 $k = -10 \rightarrow 10$
 $l = -19 \rightarrow 18$

Refinement

Refinement on F^2
Least-squares matrix: full
 $R[F^2 > 2\sigma(F^2)] = 0.040$
 $wR(F^2) = 0.111$
 $S = 1.06$
3314 reflections
190 parameters
12 restraints

Primary atom site location: structure-invariant
direct methods
Secondary atom site location: difference Fourier
map
Hydrogen site location: mixed
H-atom parameters constrained
 $w = 1/[\sigma^2(F_o^2) + (0.0521P)^2 + 1.4845P]$
where $P = (F_o^2 + 2F_c^2)/3$

$(\Delta/\sigma)_{\max} < 0.001$
 $\Delta\rho_{\max} = 0.74 \text{ e \AA}^{-3}$

$\Delta\rho_{\min} = -0.60 \text{ e \AA}^{-3}$

Special details

Geometry. All esds (except the esd in the dihedral angle between two l.s. planes) are estimated using the full covariance matrix. The cell esds are taken into account individually in the estimation of esds in distances, angles and torsion angles; correlations between esds in cell parameters are only used when they are defined by crystal symmetry. An approximate (isotropic) treatment of cell esds is used for estimating esds involving l.s. planes.

Fractional atomic coordinates and isotropic or equivalent isotropic displacement parameters (\AA^2)

	<i>x</i>	<i>y</i>	<i>z</i>	$U_{\text{iso}}^*/U_{\text{eq}}$
Br1	0.36371 (3)	0.40930 (5)	0.77766 (2)	0.05996 (15)
S1	0.27771 (6)	0.50993 (10)	0.55109 (5)	0.0478 (2)
N1	0.52247 (19)	0.7685 (3)	0.49030 (15)	0.0411 (5)
N2	0.42403 (19)	0.6853 (3)	0.48814 (15)	0.0438 (5)
N3	0.4551 (2)	0.6390 (3)	0.63168 (16)	0.0500 (6)
H3A	0.431514	0.589059	0.677388	0.060*
H3B	0.509254	0.711959	0.640888	0.060*
C1	0.3432 (2)	0.6653 (4)	0.41558 (19)	0.0467 (7)
H1A	0.380449	0.651339	0.363896	0.056*
H1B	0.295261	0.758163	0.409430	0.056*
C2	0.2763 (3)	0.5140 (4)	0.4348 (2)	0.0489 (7)
H2A	0.315568	0.419380	0.415778	0.059*
C3	0.3971 (2)	0.6205 (3)	0.56063 (18)	0.0412 (6)
C4	0.5460 (2)	0.8450 (4)	0.42487 (19)	0.0440 (6)
H4A	0.495374	0.850348	0.378264	0.053*
C5	0.6520 (2)	0.9241 (3)	0.42299 (14)	0.0416 (6)
C6	0.7284 (2)	0.9221 (4)	0.49283 (19)	0.0513 (7)
H6A	0.710541	0.874346	0.543049	0.062*
C7	0.8319 (2)	0.9924 (4)	0.4867 (2)	0.0663 (10)
H7A	0.883751	0.988871	0.532539	0.080*
C8	0.8581 (3)	1.0679 (4)	0.41226 (19)	0.0652 (10)
H8A	0.927072	1.114885	0.408687	0.078*
C9	0.7808 (2)	1.0730 (4)	0.3432 (2)	0.0651 (10)
H9A	0.797532	1.124866	0.293831	0.078*
C10	0.6782 (2)	0.9998 (4)	0.34862 (17)	0.0551 (8)
H10A	0.626928	1.001586	0.302329	0.066*
C11	0.1609 (2)	0.5115 (3)	0.39571 (17)	0.0446 (6)
C12	0.1299 (2)	0.3891 (4)	0.3387 (2)	0.0613 (9)
H12A	0.180793	0.310914	0.325946	0.074*
C13	0.0225 (2)	0.3838 (5)	0.3009 (2)	0.0690 (10)
H13A	0.002162	0.302592	0.262799	0.083*
C14	-0.0538 (3)	0.5001 (4)	0.3205 (2)	0.0661 (10)
H14A	-0.124515	0.498545	0.293897	0.079*
C15	-0.0251 (3)	0.6186 (4)	0.3794 (2)	0.0683 (10)
H15A	-0.076995	0.693888	0.394077	0.082*
C16	0.0820 (2)	0.6235 (4)	0.4163 (2)	0.0631 (9)

H16A	0.101386	0.703134	0.455623	0.076*
------	----------	----------	----------	--------

Atomic displacement parameters (\AA^2)

	U^{11}	U^{22}	U^{33}	U^{12}	U^{13}	U^{23}
Br1	0.0594 (2)	0.0700 (3)	0.0489 (2)	-0.01088 (16)	-0.00776 (15)	0.01409 (15)
S1	0.0461 (4)	0.0511 (4)	0.0467 (4)	-0.0073 (3)	0.0065 (3)	0.0068 (3)
N1	0.0379 (12)	0.0421 (13)	0.0432 (13)	-0.0028 (10)	0.0028 (10)	0.0008 (10)
N2	0.0387 (12)	0.0496 (14)	0.0429 (13)	-0.0054 (10)	0.0013 (10)	0.0085 (11)
N3	0.0544 (15)	0.0552 (15)	0.0405 (13)	-0.0076 (12)	0.0042 (11)	0.0037 (11)
C1	0.0426 (15)	0.0550 (17)	0.0418 (15)	-0.0053 (13)	-0.0020 (12)	0.0096 (13)
C2	0.0471 (16)	0.0482 (17)	0.0515 (17)	-0.0002 (13)	0.0038 (13)	-0.0012 (14)
C3	0.0406 (14)	0.0414 (14)	0.0419 (15)	0.0029 (11)	0.0062 (12)	0.0012 (12)
C4	0.0436 (15)	0.0431 (15)	0.0449 (15)	-0.0018 (12)	0.0005 (12)	0.0055 (12)
C5	0.0422 (15)	0.0334 (14)	0.0497 (16)	-0.0004 (11)	0.0063 (12)	-0.0022 (12)
C6	0.0536 (18)	0.0424 (16)	0.0566 (18)	-0.0077 (13)	-0.0055 (15)	0.0040 (14)
C7	0.053 (2)	0.055 (2)	0.087 (3)	-0.0103 (16)	-0.0162 (18)	-0.0012 (19)
C8	0.0486 (19)	0.059 (2)	0.089 (3)	-0.0127 (16)	0.0169 (19)	-0.0111 (19)
C9	0.070 (2)	0.068 (2)	0.059 (2)	-0.0205 (19)	0.0244 (18)	-0.0054 (17)
C10	0.059 (2)	0.060 (2)	0.0468 (17)	-0.0132 (16)	0.0068 (15)	-0.0005 (15)
C11	0.0407 (15)	0.0474 (16)	0.0457 (15)	-0.0051 (12)	0.0039 (12)	0.0059 (13)
C12	0.061 (2)	0.059 (2)	0.065 (2)	0.0023 (16)	0.0165 (17)	-0.0059 (17)
C13	0.063 (2)	0.082 (3)	0.061 (2)	-0.022 (2)	0.0058 (18)	-0.0193 (19)
C14	0.054 (2)	0.083 (3)	0.061 (2)	-0.0111 (19)	0.0019 (17)	0.010 (2)
C15	0.055 (2)	0.062 (2)	0.088 (3)	0.0063 (17)	0.0043 (19)	0.007 (2)
C16	0.060 (2)	0.0477 (18)	0.083 (3)	-0.0009 (15)	0.0096 (18)	-0.0116 (17)

Geometric parameters (\AA , ^\circ)

S1—C3	1.716 (3)	C6—H6A	0.9300
S1—C2	1.844 (3)	C7—C8	1.394 (2)
N1—C4	1.268 (4)	C7—H7A	0.9300
N1—N2	1.380 (3)	C8—C9	1.394 (2)
N2—C3	1.332 (4)	C8—H8A	0.9300
N2—C1	1.470 (4)	C9—C10	1.394 (2)
N3—C3	1.297 (4)	C9—H9A	0.9300
N3—H3A	0.9000	C10—H10A	0.9300
N3—H3B	0.9001	C11—C16	1.392 (2)
C1—C2	1.542 (4)	C11—C12	1.398 (2)
C1—H1A	0.9700	C12—C13	1.397 (2)
C1—H1B	0.9700	C12—H12A	0.9300
C2—C11	1.493 (4)	C13—C14	1.391 (2)
C2—H2A	0.9800	C13—H13A	0.9300
C4—C5	1.447 (4)	C14—C15	1.389 (2)
C4—H4A	0.9300	C14—H14A	0.9300
C5—C10	1.3944 (19)	C15—C16	1.390 (2)
C5—C6	1.396 (2)	C15—H15A	0.9300
C6—C7	1.395 (2)	C16—H16A	0.9300

C3—S1—C2	91.65 (14)	C5—C6—H6A	120.3
C4—N1—N2	118.4 (2)	C8—C7—C6	120.5 (3)
C3—N2—N1	116.4 (2)	C8—C7—H7A	119.8
C3—N2—C1	116.2 (2)	C6—C7—H7A	119.8
N1—N2—C1	127.4 (2)	C9—C8—C7	120.0 (3)
C3—N3—H3A	117.5	C9—C8—H8A	120.0
C3—N3—H3B	124.6	C7—C8—H8A	120.0
H3A—N3—H3B	116.8	C8—C9—C10	119.6 (3)
N2—C1—C2	105.7 (2)	C8—C9—H9A	120.2
N2—C1—H1A	110.6	C10—C9—H9A	120.2
C2—C1—H1A	110.6	C9—C10—C5	120.4 (3)
N2—C1—H1B	110.6	C9—C10—H10A	119.8
C2—C1—H1B	110.6	C5—C10—H10A	119.8
H1A—C1—H1B	108.7	C16—C11—C12	118.8 (3)
C11—C2—C1	114.9 (3)	C16—C11—C2	122.2 (2)
C11—C2—S1	111.1 (2)	C12—C11—C2	118.9 (2)
C1—C2—S1	104.1 (2)	C13—C12—C11	120.2 (3)
C11—C2—H2A	108.8	C13—C12—H12A	119.9
C1—C2—H2A	108.8	C11—C12—H12A	119.9
S1—C2—H2A	108.8	C14—C13—C12	119.9 (3)
N3—C3—N2	123.5 (3)	C14—C13—H13A	120.1
N3—C3—S1	123.1 (2)	C12—C13—H13A	120.1
N2—C3—S1	113.4 (2)	C15—C14—C13	120.4 (3)
N1—C4—C5	119.7 (3)	C15—C14—H14A	119.8
N1—C4—H4A	120.1	C13—C14—H14A	119.8
C5—C4—H4A	120.1	C14—C15—C16	119.3 (3)
C10—C5—C6	120.0 (3)	C14—C15—H15A	120.3
C10—C5—C4	118.6 (2)	C16—C15—H15A	120.3
C6—C5—C4	121.4 (2)	C15—C16—C11	121.3 (3)
C7—C6—C5	119.5 (3)	C15—C16—H16A	119.3
C7—C6—H6A	120.3	C11—C16—H16A	119.3
C4—N1—N2—C3	-173.3 (3)	C5—C6—C7—C8	1.7 (5)
C4—N1—N2—C1	4.2 (4)	C6—C7—C8—C9	-0.3 (6)
C3—N2—C1—C2	-24.6 (4)	C7—C8—C9—C10	-1.1 (6)
N1—N2—C1—C2	157.9 (3)	C8—C9—C10—C5	1.0 (6)
N2—C1—C2—C11	151.9 (3)	C6—C5—C10—C9	0.4 (5)
N2—C1—C2—S1	30.1 (3)	C4—C5—C10—C9	-177.9 (3)
C3—S1—C2—C11	-148.7 (2)	C1—C2—C11—C16	-63.2 (4)
C3—S1—C2—C1	-24.5 (2)	S1—C2—C11—C16	54.7 (4)
N1—N2—C3—N3	3.6 (4)	C1—C2—C11—C12	119.2 (3)
C1—N2—C3—N3	-174.1 (3)	S1—C2—C11—C12	-122.9 (3)
N1—N2—C3—S1	-176.5 (2)	C16—C11—C12—C13	2.5 (5)
C1—N2—C3—S1	5.8 (3)	C2—C11—C12—C13	-179.9 (3)
C2—S1—C3—N3	-168.0 (3)	C11—C12—C13—C14	-0.4 (6)
C2—S1—C3—N2	12.1 (2)	C12—C13—C14—C15	-2.1 (6)
N2—N1—C4—C5	-175.7 (3)	C13—C14—C15—C16	2.5 (6)

N1—C4—C5—C10	176.5 (3)	C14—C15—C16—C11	-0.3 (6)
N1—C4—C5—C6	-1.9 (5)	C12—C11—C16—C15	-2.1 (6)
C10—C5—C6—C7	-1.8 (5)	C2—C11—C16—C15	-179.7 (3)
C4—C5—C6—C7	176.5 (3)		

Hydrogen-bond geometry (Å, °)

D—H···A	D—H	H···A	D···A	D—H···A
N3—H3A···Br1	0.90	2.37	3.258 (3)	168
N3—H3B···Br1 ⁱ	0.90	2.55	3.399 (3)	158

Symmetry code: (i) $-x+1, y+1/2, -z+3/2$.